Journal of Applied Sciences

ISSN 1812-5654

science alert

ANSInet
an open access publisher
http://ansinet.com

Journal of Applied Sciences 7 (11): 1497-1503, 2007
ISSN 1812-5654
© 2007 Asian Network for Scientific Information

Distributions of 0.125 - 0.50 MeV/amu ^{4}He Ions Backscattered from Metallic Surface

A.A. Mahasneh, A.W. Ajlouni and O. Abu-Haija
Department of Applied Physics, Tafila Technical University, Tafila, Jordan

Abstract: A small post-accelerator has been used to measure the charge-state fractions of 0.125-0.50 MeV/amu He ions backscattered from silver films. The kinematics behavior of the backscattered ions is given by the well-known Rutherford Backscattering Spectrometry (RBS) Technique. In order to determine the film thickness at which the equilibrium film charge-state distribution occurs, we measured the charge state fractions for film thicknesses between 5.4 and 24.8 μg cm^{-2}. Deconvolution analyses of the data reveal that the charge-states of He ions backscattered from Ag-films of thickness 14.8 μg cm^{-2}, within the experimental errors, represent the equilibrium fractions. The experimental data at low energies appear to have three well-resolved peaks corresponding to the charge-state fractions of helium (He^0, He^+ and He^{++}) while at higher energies only two peaks were detected corresponding to the charge-state fractions of He^+ and He^{++}. The mean charge-state $\bar{q}$ and the width of the charge-state distribution width, d, are calculated from the Gaussian model. A formula for calculating the mean charge-state, for our studied energy range, has been proposed. The method of simultaneously measuring all charge states using a single surface barrier detector (SBD) and separation using total curve deconvolution indicates that variations in experimental conditions are minimized.

Key words: Charge fractions, mean charge, Gaussian model

INTRODUCTION

Charge-state evolution is one of the most important aspects in ion-solid interactions. Various processes, such as electron capture, ionization, excitation, vacancy production (Imai *et al*., 2005; Abufager *et al*., 2005) and the consequent phenomena like energy loss and stopping (Bentini *et al*., 2002) are closely related to the projectile charge-state evolution in the target. When energetic ions collide with a solid target, the ions undergo repeated electron-capture and electron-loss with target atoms and consequently, equilibrium of the charge-state distribution is attained for the moving ions (Arafah, 1998). The knowledge of such equilibrium charge-state distributions is of interest for a number of applications including nuclear physics, gas filled recoil separators and accelerator design (Itoh *et al*., 1999).

Charge-state fractions of backscattered ions from solid surfaces have been studied experimentally by a number of investigators. Recently, Bianconi *et al*. (2002) have obtained the equilibrium charge-state fractions of He ions transmitted from silicon in a random direction in the energy range 0.16 - 3.3 MeV. Nakajima *et al*. (2004) have carried out experimental studies of the charge-state distribution of He ions backscattered from three different surfaces; Si, SiO_2 and Ag. In their work, they obtained the dependence of the charge-state on the exit angle of the scattered ions by measuring the energy spectra for both He^+ and He^{2+} ions at various exit angles for each surface.

In this research, we report measurements of charge-state distributions of 0.125 - 0.50 MeV/amu He ions backscattered from Ag surfaces of different thicknesses (i.e., 5.4 - 24.8 μg cm^{-2}). We also perform a technique in which all charge-states fractions of backscattered ^{4}He ions are measured simultaneously in one experimental run using single surface barrier detector (SBD).

APPARATUS AND DATA ACQUISITION

Layout of the apparatus: The present measurements have been obtained on a post-accelerator (Fig. 1). $^4He^+$ ions within energy range between 0.125 and 0.50 MeV/u were produced by the 4.75 MeV Jordan University Van de Graff Accelerator (JUVAC). Then the ions were bended through a 90° angle by the analyzing magnet and guided toward the switching magnet. The selected beam was directed into a 9.5 m beam line and passed through a pair of collimators toward the scattering chamber where the interactions take place. A thin solid silver film, prepared by vacuum evaporation on silicon-wafer substrates under an applied pressure of order 10^{-4} Pa and evaporation rate of 0. 27 μg cm^{-2} s^{-1}, was mounted on a target

Corresponding Author: A.A. Mahasneh, Department of Applied Physics, Tafila Technical University, Tafila, Jordan
Tel: 00962777324574

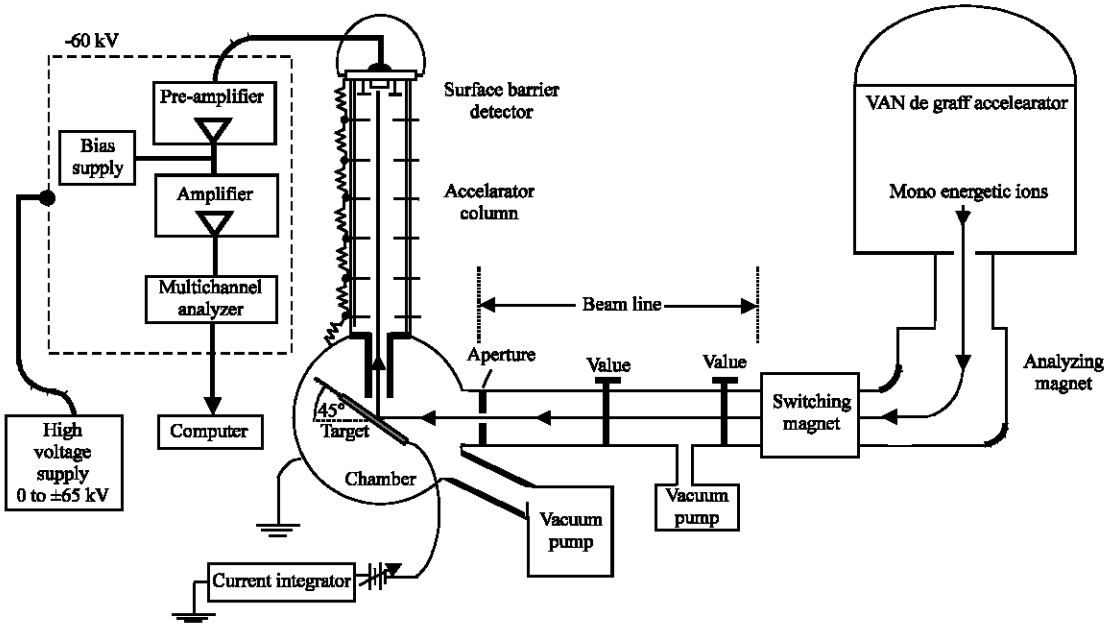

Fig. 1: Block diagram showing the experimental setup and the 60 keV post-accelerator built as a charge-state separator of backscattered ions

holder inside the scattering chamber at an angle of 45° with respect to the beam direction where the scattering geometry was chosen in such away that the beam feels the symmetrical environment along the inward and outward paths. After the collisions, the scattered ions were detected by a surface barrier detector (SBD), placed at right angle with respect to the direction of the incident beam and furnished with the necessary voltage of 60 V supplied by a bias power supply, after passing a small aperture of 1 cm in diameter located in front of the detector. The conventional electronics needed for backscattering measurements with SBD and a multichannel analyzer (MCA) were all set at negative potential relative to ground. The observations in this experimental study showed that with an additional electrostatic energy, e.g., - 60 keV (= - 0.015 MeV/amu) between the target and the SBD, the backscattered ions will gain multiples of this acceleration energy depending on their ionic charge-state n (i.e., n*60 keV). This, however, allows all charge-state fractions to be collected and measured simultaneously in one experimental run. The kinematics behavior of the backscattered ions is given by the well-known Rutherford Backscattering Spectrometry (RBS) Technique (Ziegler *et al*., 1985; Chu *et al*., 1978).

Data acquisition: Two procedures of accumulating the RBS energy spectrum were conducted. In the first procedure, energy spectrum was accumulated without post-acceleration. The spectrum is then fitted by analytical function f (E), Exponentially Modified Gaussian (EMG), which is given by Gouri and Johnson (1977):

$$f(E)=\frac{a_0}{2a_3}\exp\left(\frac{a_2^2}{2a_3^2}+\frac{a_1-E}{a_3}\right)\times\left[\operatorname{erf}\left(\frac{E-a_1}{a_2\sqrt{2}}-\frac{a_2}{a_3\sqrt{2}}\right)+\frac{a_3}{|a_3|}\right] \quad (1)$$

where a_0 is the area under the peak, a_1 is the peak center, a_2 is the width (standard deviation), a_3 is the distortion and erf is the error function. The second procedure was performed by accumulating the RBS energy spectrum with a fixed post-acceleration voltage, 60 kV in this case. As in the first procedure, the resulting spectrum is fitted by analytical function, which is the sum of weighted function f (E + nqV), according to the following relation (Arafah *et al*., 1989):

$$\left[\sum_n C_n f(E+nqV)-Y(E)\right]^2 = \text{minimum} \quad (2)$$

where f (E) is the fitted analytical function without post-acceleration voltage, E is the energy spanned over the RBS energy spectrum as obtained without post-acceleration, n is the charge state, q is the electronic charge, C_n is fitting coefficient for the n-fold charge-state

fractional contribution accelerated by an energy of nqV and Y(E) is the yield corresponding to a RBS spectrum with a fixed post-acceleration voltage V. Therefore, the charge-state fractions were determined from the total curve fitting to the postaccelerated spectra. In more details, the peak intensity, the area under the observed peak due to a certain charge-state, which is obtained from the fitted model, is a measure of its mean charge-state fraction. It is important to mention that in both procedures the obtained spectra were normalized to the same accumulated charge, i.e., the backscattering yield from a certain depth within the silicon substrate is the same, within experimental uncertainties, as that of single isolated peak without post-acceleration. Also, present study neglect the charge-state fraction of ^{4}He ions backscattered from the silicon substrate, therefore, the signals due to the silicon substrate in the obtained RBS energy spectra (with and without post-acceleration) were subtracted.

The energy dependence of the peak due to the scattering from the surface is, however, governed by the corresponding well-known kinematics equation (Arafah, 1998):

$$E(He^n) = K E_0 + nqV \quad (3)$$

where K is the RBS kinematic factor, E_0 is the incident-ion energy, n is the charge state, q is the electronic charge and V is the acceleration potential. The approach followed in separating all charge state components ensures that neither the intensity nor the peak position is disturbed by the analysis.

RESULTS AND DISCUSSION

RBS spectra of ^{4}He ions backscattered from Ag- films at impact energy of 0.188 MeV/amu: Figure 2 shows the observed RBS energy spectra for backscattered ions from the interaction of 0.188 MeV/amu ^{4}He with different silver thin film thicknesses, with and without applying post-acceleration. Also shown are the results of the fitting procedures generated by EMG model. The full width at half-maximum (FWHM) of the energy spread of the single isolated peak is about 27.6 keV (= 0.007 MeV/amu), for the thickness of 14.8 μg cm^{-2}, which is the same as those for He^0, He^+ and He^{2+}. The shape and the peak position are almost the same for all thicknesses. In addition, considerable overlapping between the charge state fractions is observed which is increased as the thickness increases. It should be mentioned that the significant overlap between the higher charge-state fractions resulting from the silicon substrate and the lower one resulting from Ag film, makes the experimental

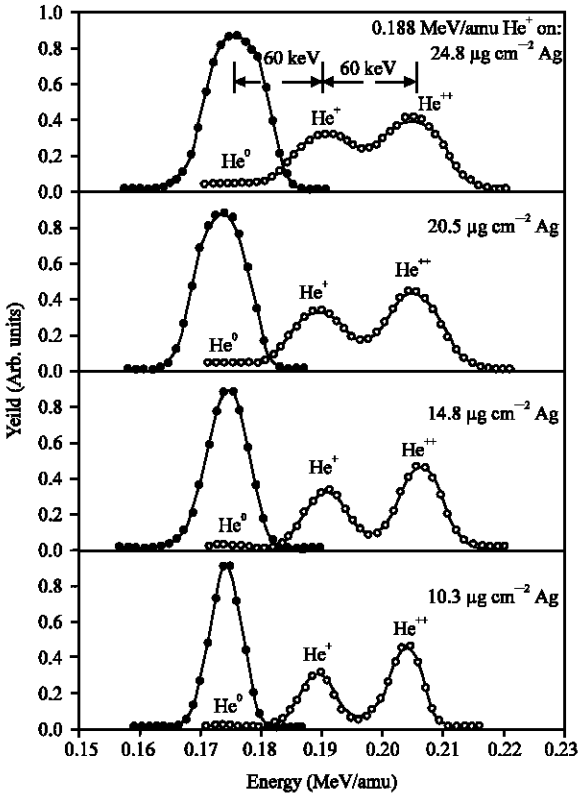

Fig. 2: The observed RBS energy spectra for ^{4}He ions backscattered from the interaction of 0.188 MeV/amu $^4He^+$ with different silver thin film thicknesses, with (o) and without (●) applying post-acceleration. The solid and dashed curves are generated data from EMG model

measurements of the fractions rather impossible. Repeated measurements were done in order to check whether the calculated fractions, backscattered from the same thickness at certain energy, changed or not. Insignificant changes were detected for some repeated measurements. However, the sharp increase of the measured neutral fractions from 7.56 to 14.64% (Table 1) could be considered due to the surface effects and non-uniformities in the deposited films. This is expected at this energy for the neutral fraction since its probability is small.

RBS spectra of ^{4}He ions backscattered from Ag-film at different impact energies: The variation of the RBS energy spectra of ^{4}He ions backscattered from 24.8 μg cm^{-2} silver films as a function of impact energy, with and without post-acceleration voltage, is shown in Fig. 3. The results also shown the fitting procedures with and without post-acceleration. At impact energy of 0.125 MeV/amu, the single isolated peak

Table 1: Equilibrium charge fractions, mean charges $\bar{q}$ and distribution width, d, for ^{4}He ions backscattered from different silver film thicknesses at various impact energies

Energy (MeV/amu)	Thickness (μg cm^{-2})	Fraction (%)			Experimental data		Gaussian distribution	
		F_0	F_1	F_3	$\bar{q}$ [(1)]	d [(2)]	$\bar{q}$ [(3)]	d[(3)]
0.125	5.40	7.56±0.80	59.76±1.10	32.68±1.34	1.25	0.57	1.27	0.61
	10.3	14.64±0.41	57.48±2.14	27.88±1.41	1.13	0.65	1.15	0.67
	14.8	8.02±0.66	63.53±1.42	28.45±0.97	1.20	0.57	1.22	0.58
	20.5	8.47±0.71	63.13±1.87	28.40±0.76	1.20	0.58	1.22	0.59
	24.8	7.32±0.99	63.42±1.71	29.26±0.81	1.21	0.57	1.23	0.58
0.188	5.40	2.22±0.65	38.66±0.67	59.12±0.31	1.57	0.62	1.58	0.62
	10.3	2.40±0.11	39.48±1.99	58.12±1.89	1.56	0.63	1.55	0.64
	14.8	2.45±0.12	39.97±0.85	57.58±1.23	1.55	0.62	1.62	0.64
	20.5	3.35±0.21	39.67±0.57	56.98±1.23	1.50	0.64	1.66	0.68
	24.8	3.67±0.23	40.00±1.02	56.33±0.76	1.53	0.63	1.66	0.66
0.250	5.40	1.46±0.12	27.33±1.60	71.21±0.97	1.70	0.66	1.71	0.64
	10.3	1.57±0.21	29.88±120	68.55±2.33	1.67	0.67	1.64	0.61
	14.8	1.30±0.08	27.62±1.24	71.08±0.88	1.66	0.66	1.66	0.65
	20.5	1.27±0.09	27.32±0.68	71.41±1.45	1.70	0.66	1.72	0.67
	24.8	0.98±0.03	27.26±1.01	71.76±0.97	1.70	0.65	1.91	0.65
0.313	5.40	0.00	16.70±0.77	83.30±2.12	1.83	0.69	1.81	0.71
	10.3	0.00	15.82±1.03	84.18±1.55	1.84	0.70	1.83	0.72
	14.8	0.00	15.36±0.36	84.64±1.59	1.85	0.69	1.88	0.66
	20.5	0.00	15.24±0.44	84.76±0.68	1.85	0.70	1.90	0.68
	24.8	0.00	15.63±0.87	84.37±2.01	1.84	0.69	1.85	0.70
0.375	5.40	0.00	11.34±0.35	88.66±1.47	1.89	0.71	1.87	0.73
	10.3	0.00	08.67±0.88	87.33±2.11	1.87	0.71	1.85	0.72
	14.8	0.00	11.86±0.42	88.14±0.87	1.88	0.72	1.90	0.70
	20.5	0.00	12.12±0.81	87.88±1.14	1.88	0.71	1.98	0.71
	24.8	0.00	11.67±0.82	88.33±1.45	1.88	0.71	1.87	0.70
0.438	5.40	0.00	07.37±0.27	92.63±1.56	1.92	0.72	1.94	0.72
	10.3	0.00	09.06±083	90.94±1.23	1.91	0.72	1.90	0.75
	14.8	0.00	08.32±0.73	91.68±0.79	1.92	0.73	1.96	0.71
	20.5	0.00	08.74±0.43	91.26±0.56	1.91	0.72	1.99	0.74
	24.8	0.00	08.25±0.64	91.75±0.69	1.92	0.72	1.93	0.71
0.500	5.40	0.00	06.48±0.86	93.52±2.11	1.93	0.73	1.95	0.78
	10.3	0.00	06.34±0.56	93.66±1.75	1.94	0.73	1.96	0.76
	14.8	0.00	07.10±0.22	92.90±1.11	1.93	0.73	1.97	0.75
	20.5	0.00	06.63±0.26	93.37±0.88	1.93	0.74	1.98	0.75
	24.8	0.00	06.81±0.12	93.19±0.95	1.93	0.73	1.99	0.77

[(1)]Calculated from Eq. 5, [(2)]Calculated from Eq. 6 and [(3)]Obtained from the Gaussian fit Eq. 4

due to ^{4}He backscattering from Ag film before applying post-acceleration splits into three distinct peak features after post-acceleration. The well-resolved peaks are corresponding to the charge-states of helium (He^0, He^+ and He^{2+}). On the other hand, at incident energies ≥0.313 MeV/amu, the peak splits into two well-resolved peaks corresponding to He^+ and He^{++}. It can be seen that the energy difference between the peaks for all charge states (i.e., peak in the spectrum without post-acceleration) and the peaks corresponding to He^+ and He^{++} is always 60 keV (= 0.015 MeV/amu). As the incident energy is increased, the doubly charged peak (fraction) increases and become dominate at incident energy ≥0.25 MeV/amu but the relative importance of the neutral and singly charged peaks (fractions) is strongly decreased. This is attributed to the fact that at low energies, the projectile ions spend enough time near the target atom and as a result their probabilities to capture an electron from the target are large (Sols and Flores, 1984). However, at higher energies, the projectile ion spends little time near the target, therefore, the interaction is swiftly completed and the projectile's electron is stripped off by the silver atom since the electrons in the conduction band do not have enough time to screen the incoming energetic ion (Goluvev *et al*., 2001; Tordoir *et al*., 2001).

Equilibrium charge-state fractions: In the Gaussian model (Stuchbery, 2006; Baudniet *et al*., 1978) the charge-state fractions is given by

$$F(q)=\frac{1}{\sqrt{2\pi d^2}}\exp\left(-\frac{(q-\bar{q})^2}{2d^2}\right) \quad (4)$$

Where q is the charge state, $\bar{q}$ is the mean charge state and d is the width of the charge-state distribution. Specifically, the mean charge-state is defined as:

$$\bar{q}=\sum_q qF(q) \quad (5)$$

However, the distribution width is denoted by:

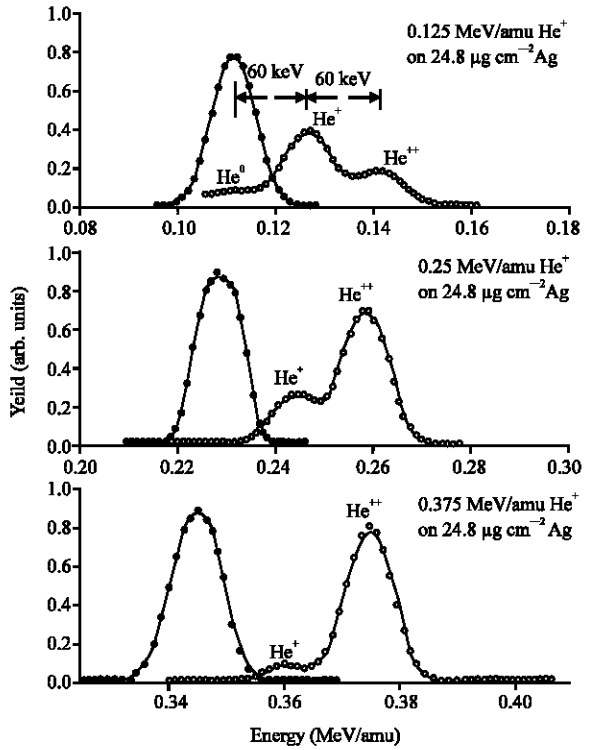

Fig. 3: The variation of the RBS energy spectra of ^{4}He ions backscattered from 24.8 μg cm^{-2} silver films at different impact energies with (o) and without (●) post-acceleration voltage. The solid and dashed curves are generated data from EMG model

$$d=\left[\sum_{q}(q-\bar{q})^2\,F(q)\right]^{1/2} \qquad (6)$$

The extracted charge-state fractions for ^{4}He ions at various energies from different silver film thicknesses, along with the relative uncertainties are listed in Table 1. In addition, $\bar{q}$ and d calculated from experimental data are also tabulated, together with those from the Gaussian fits, in Table 1. Charge-state equilibrium is, however, reached when the variation of the fraction during the passage of depth λ ceases, d F(q)/dλ→0, as λ increased. In order to determine the equilibrium charge-state fractions of backscattered ions, the thickness dependence of the charge-state fractions has to be measured (Baudinet, 1982; Lennard *et al*., 1981).

The dependence of the singly ionized helium fractions at different incident energies on the silver film thickness is displayed in Fig. 4. These fractions are reasonably constant at target thicknesses ≥ 14.8 μg cm^{-2} and fluctuate for thin thicknesses. This indicates that the measured charge-state fractions for ^{4}He ions

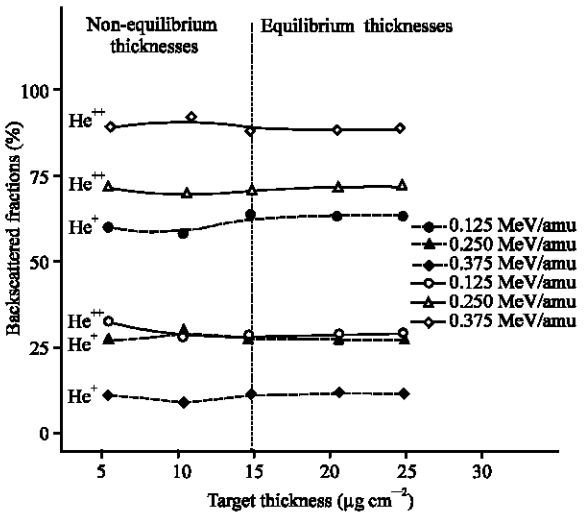

Fig. 4: The measured backscattered fractions of the charge-states He^+ and He^{++} at different impact energies plotted as a function of silver thin film thickness. Smooth solid and dashed lines are drawn to guide the eye

backscattered from 14.8 μg cm^{-2} Ag films, in the energy range studied, represent the equilibrium fractions. On the contrary, the fractions obtained from thin targets, i.e., 5.5 and 10.3 μg cm^{-2}; represent the non-equilibrium fractions since there are differences in their distributions.

Focusing Effects on the backscattered ions: The negative voltage applied to the post-accelerator is inverted to positive value. The same charge-state fractions are obtained for the same energy of the incident ions as in the case of negative value (Fig. 5). It must be emphasized that for the same accumulated charge, the integrated yield with and without post acceleration is the same. These facts exclude any significant influence on focusing the beam when the accelerated voltage is applied. Therefore, insignificant effects on the measured charge state fractions are observed. If, however, such focusing effects are present, then serious consequences could affect the accuracy of the experiment since the accelerating column would act as a series of lenses between the scattering centers and the detector system when using the accelerated configuration (Arafah *et al*., 1989).

Energy dependence of the backscattered fractions: The equilibrium charge fractions of ^{4}He ions emerging from Ag film of thickness 14.8 μg cm^{-2} are depicted as a function of projectile energy in Fig. 6. It can be seen that the measured neutral and singly charged fractions decreases with increasing impact energy. On the other hand, the

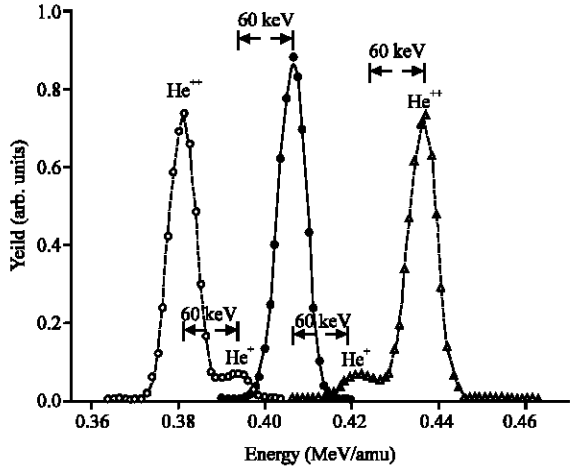

Fig. 5: RBS energy spectra of ^{4}He ions backscattered from 10.3 μg cm^{-2} silver thin film at impact energy of 0.438 MeV/amu. The experimental data without post-acceleration, with post-acceleration voltage of +60 kV and with post-acceleration voltage of -60 kV are represented by (●), (o) and (Δ), respectively. Solid, dashed and doted curves are generated data from EMG model

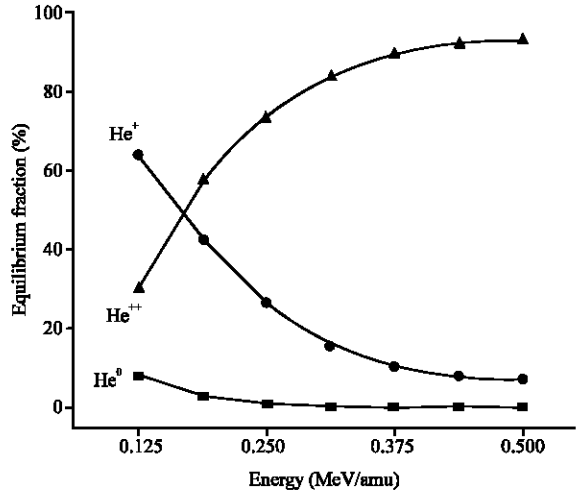

Fig. 6: The equilibrium charge fractions of ^{4}He ions emerging from Ag film of thickness 14.8 μg cm^{-2} are plotted as a function of projectile energy. The measured neutral, singly and doubly charged fractions are respectively represented by (■), (●) and (▲). Smooth solid lines are drawn to guide the eye

measured doubly charged fractions slowly increases with increasing impact energy and becomes dominant at energy above 0.188 MeV/amu.

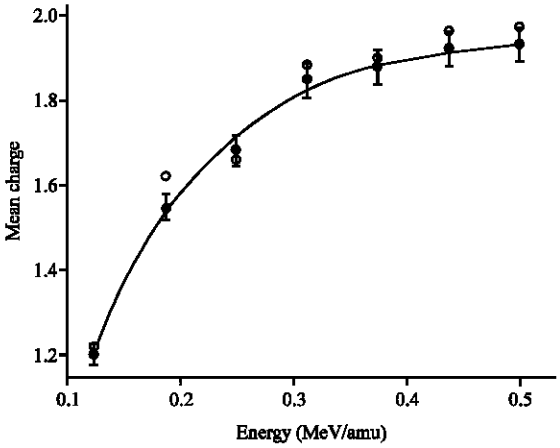

Fig. 7: Mean charge $\bar{q}$ versus energy after the backscattering. Solid circles (●) represent the experimental data from this study. The open circles (o) represent the mean charge from Gaussian fit (Eq. 4). The solid line is the exponential fit (Eq. 7). Error Bars represent the variance of the standard deviation of our measurements

Semi-empirical formula for the mean charge $\bar{q}$: Various semi-empirical or empirical formula for $\bar{q}$ of rapid ions interacting with matter have been proposed in the past (Tordoir *et al*., 2001; Itoh *et al*., 1999). Each of them is only valid within the limited domain of derivation. In our case, all available experimental data of $\bar{q}$ in the energy range 0.125- 0.50 MeV/amu are fitted by the exponential function given by:

$$Y(x) = Y_0 + A\exp\left(-\frac{(x-x_0)}{t}\right) \quad (7)$$

A good fit has been obtained (Fig. 7), where the offset, Y_0 = 194±0.0345, the center, x_0 = 0.12493±0.0034 the amplitude A = 0.763±0.0408 and the decay constant t = 0.11553±0.01668. These parameters could be physically interpreted as follows: x is the impact energy, Y(x) is the mean charge as a function of impact energy, Y_0 is the mean charge at impact energies ≥0.50 MeV/amu, x_0 is the lowest impact energy of the studied energy range. The values; x, x_0 and t are measured in MeV/amu. Figure 7 also shows the values of $\bar{q}$ obtained from the Gaussian fit (Table 1).

The inherent uncertainties arising from this work were kept at minimum level. The uncertainties are estimated within 6% in the lower probabilities, e.g., the neutral fractions at 0.188 and 0.25 MeV/amu and the singly charged fractions at 0.438 and 0.50 MeV/amu. On the other hand, the uncertainties are markedly reduced

(better than 4%) with higher fractions, e.g., doubly charged fractions at 0.375, 0.438 and 0.5 MeV/amu (Table 1).

CONCLUSIONS

We have carried out a comprehensive study of charge-state fractions of ^{4}He ions backscattered from Ag-films of different thicknesses (5.4-24.8 μg cm^{-2}) at impact energies within the range between 0.125 and 0.50 MeV/amu. The energy spectra that represent these fractions are nicely fitted by the exponentially modified Gaussian function. It turned out that the measured charge-state fractions for ^{4}He ions backscattered from 14.8 μg cm^{-2} Ag films represent equilibrium fractions. The mean charge-state $\bar{q}$ and the width of the charge state distributions, d, at different impact energies are also measured. Empirical formula for calculating the mean charge state has been proposed. The success in separating and collecting all charge-states ^{4}He ions in one measurement and their measurements using total curve deconvolution to the experimental data, both add new measurement and reliability to our determinations with the minimum inherent uncertainties due to the variations in the experimental conditions. Experiments on the angle dependence of the charge-state fractions are proposed. Furthermore, measurement of charge state fractions of ^{4}He ions at different energy ranges is, however, in progress.

REFERENCES

Abufager, P.N., A.E. Martinez, R.D. Rivarola and P.D. Fainstein, 2005. Single electron capture in ion-atom collisions involving multielectronic targets. Nucl. Instrum. Methods Phys. Res., B233: 255-259.

Arafah, D.E., J.D. Meyer, H. Sharabati and A. Mahmoud, 1989. Charge-state measurements of backscattered ions from Au films. Phys. Rev., A39: 3836.

Arafah, D.E., 1998. Equilibrium Charge state Fractions and distributiuons of ^{4}He ions backscattered from gold films. Nuovo. Cimento., 20: 261-271.

Baudniet-Robinet, Y., P.D. Dumont and H.P. Garnir, 1978. Analysis of charge-state distributions of heavy ions in carbon foils and gases. J. Phys. B: Atom. Molec. Phys., 11: 1291-1302.

Baudinet-Robinet, Y., 1982. Equilibrium charge-state distributions for heavy ions exiting carbon foils. Phys. Rev., A26: 62-71.

Bentini, G.G., E. Albertazzi, M. Bianconi, R. Lotti and G. Lulli, 2002. Charge state distribution of 3350 keV He ions channeled in silicon. Nucl. Instrum. Methods Phys. Res., B193: 113-117.

Bianconi, M., G.G. Bentini, R. Lotti and R. Nipoti, 2002. Charge state distribution of 0.16-3.3 MeV He ions transmitted through silicon. Nucl. Instrum. Methods Phys. Res., B193: 66-70.

Chu, W.K., J.W. Mayer and M.A. Nicolet 1978. Backscattering Spectrometry. Academic Press, Inc., New York.

Goluvev, A., V. Turtikov, A. Fertman, I. Roudsoky, B. Sharkov, M. Geissel, U. Neuner, M. Roth, A. Tauschwitz, H. Wahl, D.H.H. Hoffmann, U. Funk, W. Sub and J. Jacoby, 2001. Experimental investigation of the effective charge-state of ions in beam-plasma interaction. Nucl. Instrum. Methods Phys. Res., A464: 247-252.

Gouri, K. and A. Johnson, 1977. Statistical Concepts and Methods. John Wiley, New York.

Imai, M., M. Sataka, K. Kawatsura, K. Takahiro, K. Komaki, H. Shibata, H. Sugai and K. Nishio, 2005. Charge state distribution and its equilibration of 2 MeV/u sulfur ions passing through carbon foils. Nucl. Instrum. Methods Phys. Res., B230: 63-67.

Itoh, A., H. Tuschida, T. Majima, A. Yogo and A. Ogawa, 1999. Equilibrium charge distributions of lithum ions emerging from carbon foil. Nucl. Instrum. Methods Phys. Res., B159: 22-27.

Lennard, W.N., D. Philips and D.A.S. Walker, 1981. Equilibrium charge distributions of ion beam exiting carbon foils. Nucl. Instrum. Methods, 179: 413-419.

Nakajima, K., Y. Okura, M. Suzuki and K. Kimura, 2004. Charge-state distribution of 400 keV He ions scattered from solid surfaces. Nucl. Instrum. Methods Phys. Res., B219: 514-518.

Sols, F. and F. Flores, 1984. Charge transfer processes for light ions moving in metals. Phys. Rev., B30: 4878-4880.

Stuchbery, A.S., A.N. Wilson and P.M. Davidson, 2006. Equilibrium charge-state distributions for S and Si ions emerging from iron and gadolinium targets with velocities near their K-shell electron velocity. Nucl. Instrum. Methods Phys. Res., B243: 265-271.

Tordoir, X., T. Bastin, P.D. Dumont and H.P. Garinir, 2001. Equilibrium charge-state distributions of sodium ions in carbon foil. Nucl. Instrum. Methods Phys. Res., B173: 275-280.

Ziegler, J.F., J.P. Biersack and N. Littmark, 1985. The Stopping and Range of Ions in Solids. Pergamon Press, New York.